Efficient Autoionization Following Intense Laser-Cluster Interactions

B. Schütte,[1,2,*] J. Lahl,[3] T. Oelze,[3] M. Krikunova,[3] M. J. J. Vrakking,[1] and A. Rouzée[1]
[1]Max-Born-Institut, Max-Born-Strasse 2A, 12489 Berlin, Germany
[2]Department of Physics, Imperial College London, South Kensington Campus, SW7 2AZ London, United Kingdom
[3]Institut für Optik und Atomare Physik, Technische Universität Berlin, Hardenbergstr 36, ER 1-1, 10623 Berlin, Germany
(Received 21 November 2014; revised manuscript received 23 January 2015; published 24 March 2015)

Electron emission as a result of the interaction of clusters with intense laser pulses is commonly understood in terms of direct and evaporative ionization processes. In contrast, we provide evidence here of an important role played by autoionization in intense field ionization of molecular oxygen clusters. Superexcited states are populated during the cluster expansion, and their autoionization is observed on a ns time scale. Decay processes on fs to ps time scales are obscured by energy exchange of the emitted electrons with the environment.

DOI: 10.1103/PhysRevLett.114.123002 PACS numbers: 32.80.Rm, 32.80.Zb, 36.40.-c, 52.50.Jm

Strong-field ionization of atomic and molecular clusters with near-infrared (NIR) light pulses has been the subject of intensive research in the last two decades and has revealed very interesting processes that are absent in isolated atoms and molecules. Among these, the acceleration of ions [1] and neutral atoms [2] to MeV kinetic energies has been reported. When molecular clusters are exposed to light pulses at very high intensities, the large absorbed laser energy can even lead to nuclear fusion [3].

These processes become possible because of very efficient electron impact ionization processes in clusters that are driven by strong internal fields and that can dominate over multiphoton and tunneling ionization [4]. Most of the generated electrons remain trapped inside the cluster, where a nanoplasma is formed [5]. These quasifree electrons undergo many collisions leading to a quick thermalization. In previous experiments, the electron spectrum obtained from clusters ionized by intense NIR pulses showed a smooth kinetic energy distribution [6,7], explained both in terms of direct electron emission and electron evaporation from the nanoplasma [4]. Most of the existing models describing the dynamics of laser-generated nanoplasmas in clusters do not take into account transitions from continuum to excited bound states and vice versa [4,5,8]. In plasmas, these transitions play an important role though, as is, e.g., known for astronomical plasmas [9]. In the case of clusters, a significant population of high-lying Rydberg states [10] and low-lying excited states [11,12] attributed to efficient electron-ion recombination processes occurring in the nanoplasma was recently reported both in the NIR and extreme-ultraviolet (XUV) regimes.

One process that can strongly influence the cluster relaxation dynamics and the observed charge state distributions and that, so far, has not been considered to be important in intense NIR laser-cluster ionization is autoionization [13,14], a multielectron process where energy exchange between several bound electrons leads to the ionization of one of them. Considering the important role of recombination encountered in our earlier studies [10–12], a substantial population of autoionizing states may be anticipated when a cluster is driven to a suitably high degree of ionization. The identification of autoionization in cluster experiments is challenging though, due to the strong interaction of the generated electrons with the charged cluster environment, which alters their kinetic energies with respect to the energies that would be observed under field-free conditions. As a result, no published reports on the occurrence of autoionization in the interaction of intense NIR laser pulses with clusters exist.

In this Letter, we report on the observation of extensive autoionization in O_2 clusters that are ionized by intense NIR laser pulses. During the cluster expansion, large amounts of superexcited oxygen atoms are populated. In the experiment, we directly observe their autoionization on a ns time scale. Faster autoionization likely occurs as well, but cannot be explicitly observed due to the energy exchange of the produced electrons with the cluster environment. On the basis of our results, we conclude that autoionization following significant excited state population is of high importance for the understanding of ion charge-state distributions observed from clusters [15–17] and large molecules [18] at different ionization wavelengths. The reason is that very different initial ionization processes in the XUV and NIR regimes are followed by very similar subsequent nanoplasma relaxation dynamics [10–12].

Nanoplasmas are commonly modeled by considering the atoms, ions, and electrons as classical particles, whereas their quantum properties are neglected. Our experimental results show that quantum mechanical phenomena such as autoionization resulting from electron correlation may significantly modify the final experimental observables that numerical models can compare to and, thus, have to be suitably included in the theory.

The experimental setup is schematically shown in Fig. 1. We use a 50 Hz Ti:Sapphire laser amplifier operating at a central wavelength of 790 nm and delivering a pulse energy up to 35 mJ and a pulse duration of 32 fs at full width half maximum [19]. The stretched NIR beam is split before compression by a beam splitter that is located in the amplifier system. After compression, the reflected part is focused into the interaction zone using a spherical mirror with a focal length of 75 mm. Here, it is crossed at right angles by a cluster beam that is generated by a piezoelectric valve with a 0.5 mm diameter nozzle. The central part of the cluster beam is selected by a 0.2 mm molecular beam skimmer. The average cluster size in the experiments is estimated as $\langle N \rangle = 2400$ molecules according to the Hagena scaling law [20], using a value of 1400 for the gas parameter k [21]. Electrons and ions generated by the laser-cluster interaction are detected with a velocity map imaging (VMI) spectrometer [22]. From the recorded 2D momentum distributions, we obtain kinetic energy spectra by means of an Abel inversion method [23].

An interferometric setup is employed for the NIR-NIR pump-probe-experiment. The NIR probe beam that is transmitted by the aforementioned beam splitter and that is compressed by a second compressor is recombined with the NIR pump beam using a mirror with a 6 mm central hole that reflects the outer part of the probe beam, while the pump beam is transmitted through the hole. From this point, both beams collinearly copropagate towards the focusing mirror. The intensities of both pump and probe beams can be adjusted with the help of irises and neutral density filters.

In order to obtain insight into the electron emission characteristics from O_2 molecules and O_2 clusters, we recorded angle-resolved electron momentum spectra upon NIR ionization using an intensity of 9×10^{13} W/cm^2. In the case of isolated molecules, a strongly anisotropic electron emission with a dominant contribution along the laser polarization direction is observed [Fig. 2(a)]. The well-resolved broader peaks in the angle-integrated kinetic energy distribution [Fig. 2(b)] separated by the NIR photon energy of 1.57 eV are due to above-threshold ionization,

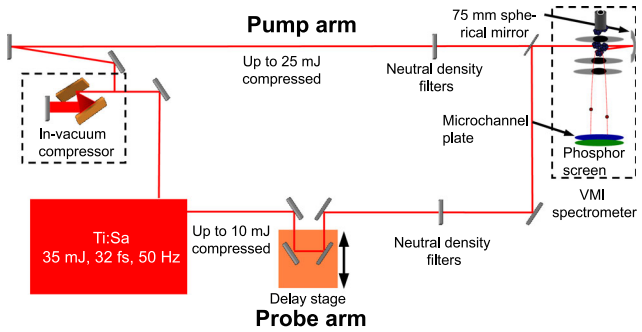

FIG. 1 (color online). Experimental scheme for the NIR-NIR pump-probe measurement. See text for details.

while the narrow peaks visible below 1.5 eV are attributed to Freeman resonances that are induced by ponderomotive shifts of bound states [24]. In contrast, the electron emission from O_2 clusters displayed in Fig. 2(c) is almost isotropic. The angle-integrated kinetic energy spectrum in Fig. 2(d) reveals a clear peak structure on top of a smooth electron energy distribution. This structure is highly surprising, since, in NIR-induced cluster explosions, extensive interaction of all electrons and ions inside the cluster usually leads to a disappearance of any bound-state signatures in the final electron spectrum. The observation of sharp peaks in the electron kinetic energy distribution directly allows one conclusion to be drawn about the origin of the electrons: At the time of electron emission, the cluster potential must be negligible, since the peaks would, otherwise, be smeared out (cf. [11]). Therefore, the sharp electron emission must either take place very early during the laser pulse or long after the laser pulse has ended, when the cluster has significantly expanded and the cluster potential is correspondingly small. The former explanation is unlikely though, since one would then expect the ejected electrons to be accelerated by the laser field, leading to a peaked angular distribution [like in Fig. 2(a)], in contrast with the experimental observation in Fig. 2(c). We, therefore, conclude that the peaks are due to the population of excited states that decay via autoionization during an advanced stage of the cluster fragmentation.

Autoionization of atomic and molecular oxygen has been extensively studied in the past [25–29], allowing for

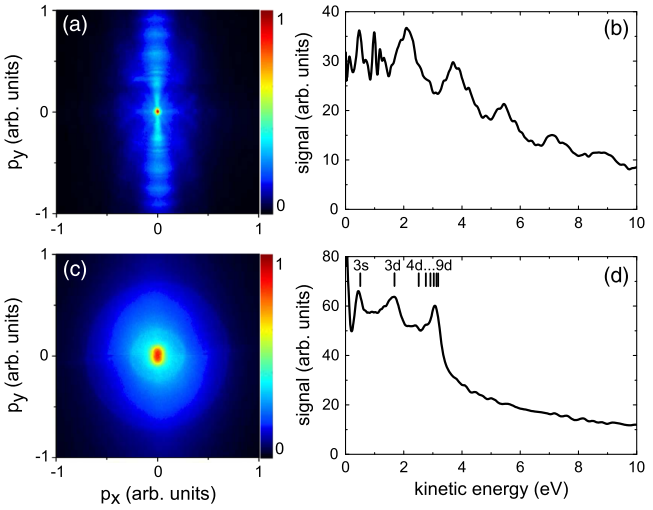

FIG. 2 (color online). (a) 2D momentum map of O_2 molecules at an NIR intensity of 9×10^{13} W/cm^2 and (b) the corresponding angle-integrated photoelectron spectrum. (c) 2D momentum map of O_2 clusters with an average size of $\langle N \rangle = 2400$ molecules at the same NIR intensity. (d) Peaks in the angle-integrated kinetic energy spectrum are attributed to autoionization processes of superexcited oxygen atoms formed during the cluster expansion. The $2s^2 2p^3 (^2P^o) 3s (^3P^o)$ state and the first states of the $2s^2 2p^3 (^2D^o_{3/2}) nd (^3P^o)$ series are marked.

a straightforward identification of the observed peaks. In Fig. 2(d), the peak at an energy of 0.5 eV is attributed to autoionization from the $2s^2 2p^3(^2P^o)3s(^3P^o)$ superexcited state of atomic oxygen that was labeled as $A2$ in [29]. Similarly, the peak at 1.7 eV is identified as the $2s^2 2p^3(^2D^o{}_{3/2})3d(^3P^o)$ state labeled as $A5$. The peak around 3 eV is due to an overlap of several autoionizing states that become more dense towards higher energies [27]. Autoionization of these states takes place on a time scale of 1 ns [28], where the cluster has dissociated into individual fragments. We note that, in this case, autoionization competes with fluorescent decay, for which similar rates have been reported [28]. We further note that, similar to the findings in oxygen, we have observed autoionization in krypton and xenon clusters as well.

Experimental rates for the observed autoionization processes can be estimated by performing an NIR-NIR pump-probe experiment, where a pump pulse triggers the cluster ionization and where a probe pulse depopulates the excited states, suppressing the autoionization. A drawback of this method is that the weak probe pulse also reionizes lower excited atoms that are formed by electron-ion recombination (EIR) processes during the cluster expansion, producing additional peaks in the low-energy part of the electron kinetic energy distribution. In Fig. 3(a), we show electron kinetic energy spectra recorded perpendicular to the laser, where the contribution of electrons from these lower excited states is less pronounced, since these exhibit an anisotropic distribution with a maximum signal along the laser polarization. In Fig. 3(a), the observed peaks become sharper for larger pump-probe time delays, a behavior that reflects the decreasing influence of the cluster potential on the generated electrons as the cluster expands.

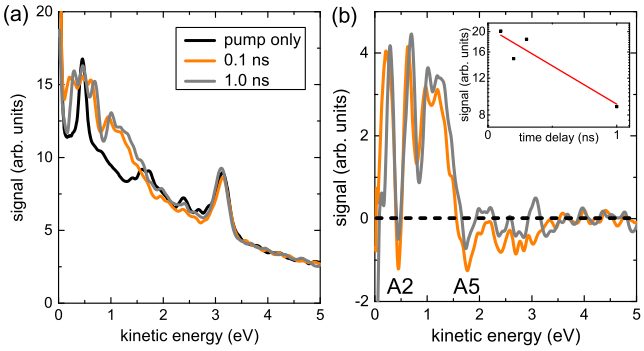

FIG. 3 (color online). (a) Electron kinetic energy spectra from O_2 clusters taken at different time delays between two NIR pulses with intensities of 9×10^{13} and 5×10^{12} W/cm^2. The pump and probe pulses have a duration of 32 fs and 1 ps, respectively. The spectra show the emission in perpendicular direction to the laser polarization and were normalized with respect to the signal obtained in the range between 4 and 5 eV, where no influence from the probe pulse is expected. (b) Difference spectra of the spectra in (a), where the signal from the pump pulse only was subtracted from the signal obtained in the pump + probe experiment. The negative signal at the $A2$ and $A5$ peaks is attributed to the suppression of autoionization by the probe pulse. The inset shows the autoionization signal integrated between 1.65 and 1.85 eV for different time delays. From the exponential fit, an autoionization lifetime of about 1 ns is obtained.

In Fig. 3(b), the difference between two measurements obtained in the pump + probe experiment and an experiment with the pump pulse only is presented. At 0.5 and 1.7 eV, where the $A2$ and $A5$ peaks were identified, the signal becomes negative, suggesting that the autoionization is partially suppressed by the probe laser pulse. The suppression of autoionization becomes less pronounced when changing the time delay from 0.1 to 1 ns. This is shown in the inset of Fig. 3(b) for the $A5$ peak, where an autoionization lifetime of about 1 ns is obtained, in reasonable agreement with lifetime measurements of these states [26,28]. According to [28], ns-scale autoionization processes occur when the autoionization process is LS forbidden, where L is the total orbital angular momentum and S is the total spin. Thus, it is expected that in addition to the autoionization processes that we can detect in our experiment, LS-allowed ionization processes occur on shorter (fs to ps) time scales, further underscoring the importance of autoionization phenomena during and after the cluster excitation.

While we cannot unambiguously deduce the mechanism for the population of the autoionizing states from the experiment, we provide, in the following, a discussion of different possible pathways. We mostly consider scenarios involving oxygen atoms, where the formation of highly excited autoionizing states can result from the interaction of one or more continuum electrons with an O^{2+} ion, an O^+ ion, or a neutral O atom. Since autoionization (AI) peaks are not observed in strong-field ionization of isolated oxygen atoms or molecules, we exclude direct excitation by multiple photons and consider the following processes:

$$2e^- + O^{++} \xrightarrow{\text{TBR}} e^- + O^{+*} \xrightarrow{\text{TBR}} O^{**} \xrightarrow{\text{AI}} e^- + O^+, \quad (1)$$

$$e^- + O^{+*} \xrightarrow{\text{TBR}} O^{**} \xrightarrow{\text{AI}} e^- + O^+, \quad (2)$$

$$e^- + O^+ \xrightarrow{\text{DR}} O^{**} \xrightarrow{\text{AI}} e^- + O^+, \quad (3)$$

$$e^- + O \xrightarrow{\text{EIE}} O^{**} \xrightarrow{\text{AI}} e^- + O^+. \quad (4)$$

In case (1), a sequence of two three-body recombination (TBR) [30] events produces a doubly excited neutral atom, which autoionizes as a result of energy exchange between two electrons that have recombined into excited states. During TBR, the excess energy of the recombining electron needs to be transferred to a quasifree electron in the vicinity. TBR, in particular, is possible at higher plasma densities (during earlier times of the cluster expansion). In case (2), the doubly excited autoionizing state is formed

by a single TBR process in an ion that is already excited, e.g., by electron impact excitation (EIE). In case (3), known as dielectronic recombination (DR) and involving a two-body collision between an electron and a singly ionized atom, a bound electron gets excited by the excess energy of the recombining electron, resulting in a doubly excited neutral atom that autoionizes [13,14]. Finally, in case (4), the EIE process involves a collision of a neutral atom and a continuum electron, and two electrons get excited in the process. We note that EIE processes are most efficient during the interaction of the laser pulse with the cluster. By contrast, EIR takes place on a ps time scale [11]. More complicated processes are possible when the formation of the autoionizing neutral atom involves a highly excited state of the molecule as an intermediate.

The data in Figs. 2 and 3 represent an exceptional situation, where autoionization peaks can be clearly observed in the photoelectron spectra, and an assignment to specific states is possible. In the following, we demonstrate that, in general, little structure is observed in the electron spectra, even though autoionization takes place. When the NIR intensity is reduced to 7×10^{13} W/cm^2 [Fig. 4(a)], the spectrum shows a smooth behavior. In this measurement, the strong contribution of very low-kinetic-energy electrons in the meV range (marked by the arrow) is attributed to a frustrated recombination process [10,31], where the dc detector electric field ionizes highly excited Rydberg atoms that are formed by EIR. Only a weak contribution from the $A2$ autoionization channel is observed at this intensity, which is in accordance with the dominant O_2^+ contribution in the ion time-of-flight (TOF) spectrum (see inset) and the interpretation that autoionization takes place in atomic oxygen. At an intensity

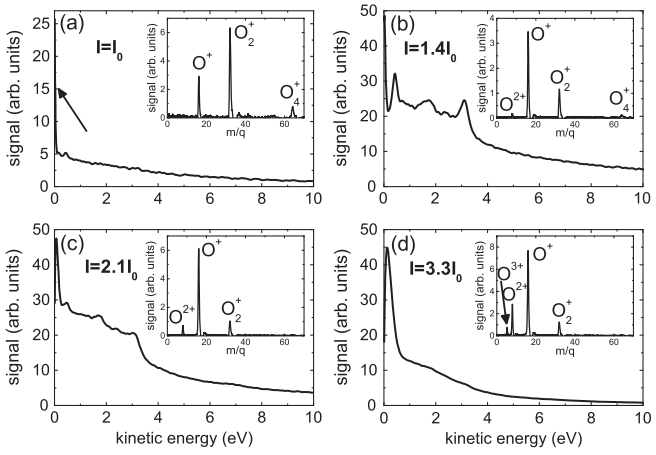

FIG. 4. Electron kinetic energy spectra from O_2 clusters at different NIR intensities of (a) 7×10^{13} W/cm^2, (b) 9×10^{13} W/cm^2, (c) 1.4×10^{14} W/cm^2, and (d) 2.3×10^{14} W/cm^2. The arrow in (a) marks the low-kinetic energy distribution attributed to frustrated recombination. The insets show the corresponding ion TOF spectra for each intensity.

of 9×10^{13} W/cm^2 [Fig. 4(b)], a clear structure of autoionization peaks appears, in agreement with the dominant O^+ contribution in the TOF spectrum. The autoionization peak structure remains visible, but is smeared out at an intensity of 1.4×10^{14} W/cm^2 [Fig. 4(c)]. This is explained by a larger cluster charge at the higher intensity and a correspondingly increased cluster potential at the time of autoionization, leading to a kinetic energy downshift of the electrons. The peaks are hardly discernible at an intensity of 2.3×10^{14} W/cm^2 [Fig. 4(d)], although the distribution is still clearly nonexponential and hints of the peaks near 1.7 and 3 eV remain. Instead, a large signal is observed below 0.5 eV due to an increased energy downshift of the electrons. We note that the electron and ion signals are increased by 2 orders of magnitude when increasing the NIR intensity from 7×10^{13} to 2.3×10^{14} W/cm^2. Because of this high nonlinearity, we expect that most of the detected electrons and ions are generated in the region of the highest NIR intensity. When the intensity is changed from 9×10^{13} to 2.3×10^{14} W/cm^2, the average kinetic energy of the detected electrons decreases, as observed in Fig. 4. This is in contrast to a picture, where the measured electron distribution has a higher temperature at higher intensities. Instead, this behavior supports the persistence of substantial autoionization contributing to the cluster ionization.

In addition to the observed autoionization taking place on a ns time scale, many autoionizing states with ps decay times exist and were observed in previous experiments on atomic and molecular oxygen [25,28,29]. We, therefore, expect these states to be populated in substantial amounts during the cluster expansion, even though their signatures are not observable in the kinetic energy spectra. Further autoionization processes are known to take place on a fs time scale [32]. These fast processes can strongly influence the cluster relaxation dynamics. For instance, the charge state distributions can be heavily modified by autoionization processes. For an accurate description of nanoplasma dynamics, autoionization processes have to be included in future model calculations.

In summary, we have demonstrated an efficient autoionization process following the ionization of oxygen clusters by intense NIR pulses. We attribute this observation to the decay of superexcited oxygen atoms on ns time scales. It is shown that spectral autoionization signatures vanish at higher intensities due to the energy exchange of the emitted electrons with the charged cluster environment. Further autoionization processes may take place on ps and sub-ps time scales. Based on the results presented in this Letter, we expect autoionization to be of general importance in extended systems such as atomic clusters or large molecules, following an extensive formation of multiply excited atoms and ions at sufficient laser intensities. The current results are in contrast to models that are commonly

used to describe the electron emission from clusters interacting with intense light pulses that completely neglect bound-continuum state transitions.

M. K., T. O., and J. L. acknowledge financial support by the BMBF Project No. 05K13KT6.

*schuette@mbi-berlin.de

[1] T. Ditmire, J. W. G. Tisch, E. Springate, M. B. Mason, N. Hay, R. A. Smith, J. Marangos, and M. H. R. Hutchinson, Nature (London) **386**, 54 (1997).
[2] R. Rajeev, T. Madhu Trivikram, K. P. M. Rishad, V. Narayanan, E. Krishnakumar, and M. Krishnamurthy, Nat. Phys. **9**, 185 (2013).
[3] T. Ditmire, J. Zweiback, V. P. Yanovsky, T. E. Cowan, G. Hays, and K. B. Wharton, Nature (London) **398**, 489 (1999).
[4] T. Fennel, K.-H. Meiwes-Broer, J. Tiggesbäumker, P.-G. Reinhard, P. M. Dinh, and E. Suraud, Rev. Mod. Phys. **82**, 1793 (2010).
[5] T. Ditmire, T. Donnelly, A. M. Rubenchik, R. W. Falcone, and M. D. Perry, Phys. Rev. A **53**, 3379 (1996).
[6] Y. L. Shao, T. Ditmire, J. W. G. Tisch, E. Springate, J. P. Marangos, and M. H. R. Hutchinson, Phys. Rev. Lett. **77**, 3343 (1996).
[7] E. Springate, S. A. Aseyev, S. Zamith, and M. J. J. Vrakking, Phys. Rev. A **68**, 053201 (2003).
[8] U. Saalmann, C. Siedschlag, and J. Rost, J. Phys. B **39**, R39 (2006).
[9] G. J. Ferland, K. T. Korista, D. A. Verner, J. W. Ferguson, J. B. Kingdon, and E. M. Verner, Publ. Astron. Soc. Pac. **110**, 761 (1998).
[10] B. Schütte, M. Arbeiter, T. Fennel, M. J. J. Vrakking, and A. Rouzée, Phys. Rev. Lett. **112**, 073003 (2014).
[11] B. Schütte, F. Campi, M. Arbeiter, T. Fennel, M. J. J. Vrakking, and A. Rouzée, Phys. Rev. Lett. **112**, 253401 (2014).
[12] B. Schütte, T. Oelze, M. Krikunova, M. Arbeiter, T. Fennel, M. J. J. Vrakking, and A. Rouzée, New J. Phys. (in press).
[13] M. B. Smirnov and W. Becker, Phys. Rev. A **69**, 013201 (2004).
[14] V. P. Krainov and A. V. Sofronov, J. Exp. Theor. Phys. **103**, 35 (2006).
[15] E. M. Snyder, S. A. Buzza, and A. W. Castleman, Phys. Rev. Lett. **77**, 3347 (1996).
[16] H. Wabnitz *et al.*, Nature (London) **420**, 482 (2002).
[17] T. Gorkhover *et al.*, Phys. Rev. Lett. **108**, 245005 (2012).
[18] B. F. Murphy *et al.*, Nat. Commun. **5**, 4281 (2014).
[19] G. Gademann, F. Ple, P.-M. Paul, and M. J. J. Vrakking, Opt. Express **19**, 24922 (2011).
[20] O. F. Hagena, Surf. Sci. **106**, 101 (1981).
[21] R. A. Smith, T. Ditmire, and J. W. G. Tisch, Rev. Sci. Instrum. **69**, 3798 (1998).
[22] A. T. J. B. Eppink and D. H. Parker, Rev. Sci. Instrum. **68**, 3477 (1997).
[23] M. Vrakking, Rev. Sci. Instrum. **72**, 4084 (2001).
[24] R. R. Freeman, P. H. Bucksbaum, H. Milchberg, S. Darack, D. Schumacher, and M. E. Geusic, Phys. Rev. Lett. **59**, 1092 (1987).
[25] A. S. Sandhu, E. Gagnon, R. Santra, V. Sharma, W. Li, P. Ho, P. Ranitovic, C. L. Cocke, M. M. Murnane, and H. C. Kapteyn, Science **322**, 1081 (2008).
[26] G. M. Lawrence, Phys. Rev. A **2**, 397 (1970).
[27] P. M. Dehmer, J. Berkowitz, and W. A. Chupka, J. Chem. Phys. **59**, 5777 (1973).
[28] P. M. Dehmer, W. L. Luken, and W. A. Chupka, J. Chem. Phys. **67**, 195 (1977).
[29] R. Feifel, J. H. D. Eland, and D. Edvardsson, J. Chem. Phys. **122**, 144308 (2005).
[30] E. Hinnov and J. G. Hirschberg, Phys. Rev. **125**, 795 (1962).
[31] T. Fennel, L. Ramunno, and T. Brabec, Phys. Rev. Lett. **99**, 233401 (2007).
[32] S. Gilbertson, M. Chini, X. Feng, S. Khan, Y. Wu, and Z. Chang, Phys. Rev. Lett. **105**, 263003 (2010).